ANALYSIS OF COMPOSITE STRUCTURES WITH DELAMINATIONS UNDER COMBINED BENDING AND COMPRESSION[1]

Han-Pin Kan
Northrop Corporation, Aircraft Division
Hawthorne, California

Edward Kautz
Naval Air Development Center
Warminster, Pennsylvania

Larry Neri
FAA Technical Center
Atlantic City Airport, New Jersey

ABSTRACT

A methodology has been developed for strength prediction of composite structures with delaminations under combined bending and compression loads. The methodology is an extension of the delamination analysis method developed under the USAF/Boeing/Northrop "Damage Tolerance of Composites" program. Delamination buckling and strain energy release rate analyses are used as basic tools in the strength prediction. In addition, failure mode interaction and structural configuration effects are taken into consideration. The influence of fasteners on the strength of a delaminated structure is incorporated to evaluate assembly-caused delaminations. The capabilities and limitations of the analysis method are demonstrated by correlating the analytical results with existing experimental data. The failure load, failure mode and failure sequence of a structure containing delaminations are predicted and the analytical results are compared with test data.

INTRODUCTION

The current trend in aircraft design is to use advanced composite materials in primary and secondary structure, wherever possible, in order to reduce weight and increase performance. During assembly of these structures, interply delamination of composites can occur. When an assembly utilizes bolts, for example, delaminations can occur when torquing the bolts causes mating parts to be forced together due to the existence of an unshimmed gap between those parts. Delaminations occurring during final assembly are of particular concern because final assemblies are not generally subjected to non-destructive inspection, and, even if an inspection is performed, not all areas are accessible after final assembly. These delaminations can cause

1 This work was performed under NADC/FAA/Northrop Contract N62269-90-C-0282, entitled "Delamination Methodology for Composite Structures."

significant reduction in the load carrying capability of structure, particularly in compression strength and in the strength of structure subjected to out-of-plane loading. In addition, there is a potential for delamination growth under fatigue loading, which can further reduce load carrying capabiity. Therefore, it is very important to have a validated methodology for assessing the severity of known delaminations with respect to their effects on strength and life so repair/replacement decisions can be made.

In recent years, considerable effort has been devoted to the development of delamination analysis methods for composite structures. These analyses have been of two types: (1) one-dimensional analyses for through-the-width delaminations in composite structural members and (2) two-dimensional analyses that focus on a delaminated region in a composite plate. The two-dimensional analyses have been developed for specialized delamination geometries (e.g., circular, elliptical, or rectangular delaminations).

One-dimensional analysis methods are given in References 1 through 9. With the exception of References 2 and 6, which are based on a finite element approach, each of the one-dimensional methods provides closed-form results using a beam-column model. Two-dimensional delamination analysis methods are given in References 1 and 10 through 19. References 14, 15, and 18 are based wholly or partially upon finite element analysis. The remaining analyses are based upon classical plate methods or Rayleigh-Ritz approaches applied to circular or elliptical delaminations in a composite panel.

The effects of delamination on the static strength and fatigue life are experimentally examined in References 1, 3, 4, 10 and 20 through 23. An extensive database was generated in Reference 1. The parameters investigated in this reference include material, test environment, laminate thickness and layup, delamination size and location, and structural configuration. A systematic review of experimental data was also conducted in Reference 1.

The objective of the present paper is to develop an analysis method for strength and failure mode prediction of composite structures containing assembly caused delaminations. To achieve this objective, the methodology developed in Reference 1 is first extended to include the effects of out-of-plane bending on the strength of delaminated composite laminate. This analysis method is then modified to accommodate the presence of a hole and a torque-up fastener.

ANALYSIS DEVELOPMENT

The analysis method developed in Reference 1 is used in the present work as a baseline methodology. In the reference, a three-part analysis was developed. These are: (1) delamination buckling analysis, (2) strain-energy-release-rate computation, and (3) failure predictions. This analytical procedure is discussed in the following paragraphs.

Delamination Buckling Analysis

Laminate with an Elliptical Delamination Subjected to Combined Bending and Compression Loads. Consider a composite laminate with an elliptical delamination subjected to combined bending moment and axial compression as shown in Figure 1. The delaminated layer (layer 1 in the figure) consists of n plies with thickness t_1. This layer is treated as a thin, elastic, orthrotropic, elliptical plate with major and minor axes a and b, respectively. The plate boundary is considered to be between simply supported and fully clamped. A boundary fixity coefficient $0.0 \leq \alpha \leq 1.0$ is used to describe the boundary condition. The value of α is 0 when the boundary is fully clamped and $\alpha = 1.0$ for a simply supported boundary.

Under combined loading, the strain due to axial force (ϵA) and the strain due to bending moment (ϵB) are obtained from the classical lamination theory. These strains are given by

$$\epsilon A = \frac{N}{A_{11}} \tag{1}$$

and

$$\epsilon B = \frac{My}{D_{11}} \tag{2}$$

where M is the bending moment per unit width of the laminate
N is the axial compression per unit width of the laminate
A_{11} is the axial stiffness of the laminate
D_{11} is the bending rigidity of the laminate
y is the distance from the neutral axis of the laminate to the point of interest

The buckling load of the delaminated layer is obtained using the method of Reference 1 and is given by:

$$N_{crd} = \frac{1}{a^2}\left[(12-8\alpha)D_{11d} + 8\left(\frac{a}{b}\right)^2 D_{12d} + (12-8\alpha)\left(\frac{a}{b}\right)^4 D_{22d} + 16\,(1-\alpha)\left(\frac{a}{b}\right)^2 D_{66d}\right] \tag{3}$$

where D_{11d}, D_{12d}, D_{22d} and D_{66d} are the bending rigidities of the delaminated layer.

The buckling load of the delaminated layer is obtained by equaling the total force in the layer to the critical load given in equation (3).

The total force in the delaminated layer is computed by summing the forces in each ply of the layer. This force is given by

$$N_d = \frac{N}{A_{11}} \Sigma A_{11i} + \frac{M}{D} \Sigma A_{11i} y_i \tag{4}$$

where the summation is over the n_d plies.

At buckling $N_d = N_{crd}$, or the right hand side of equation (3) is equal to the right hand side of equation (4).

Laminate with an Elliptical Delamination Around A Fastener Subjected to Combined Bending and Compression Loads. A second delamination configuration considered here is used to simulate the assembly-caused delamination in built-up composite structures. The delamination configuration considered is illustrated in Figure 2. The analysis method is an extension of the energy method developed in Reference 1. The displacement function for the current method is assumed to be

$$w = A \left(1 - \frac{x^2}{a^2} - \frac{y^2}{b^2}\right)^2 \left(1 - \frac{x^2+y^2}{R^2}\right)^2 \tag{5}$$

where

A is an undefined coefficient

a and b are the major and minor axes of the elliptical delamination

R is the radius of the fastener hole

The displacement function defined in equation (5) represents a simply supported boundary around the delamination as well as around the hole. Thus, the clamp-up effect of the fastener head is conservatively approximated by the zero displacement around the hole. With this displacement function, the buckling load can be determined by the energy method. The strain energy is given by

$$U = \frac{1}{2} \int\int \left[D_{11} w^2_{xx} + 2D_{12}\, w_{xx}\, w_{yy} + D_{22}\, w_{yy}^2 + 4D_{66}\, w_{xy}^2\right] dxdy \tag{6}$$

where

D_{11}, D_{22}, D_{12}, and D_{66} are the plate (delamination) bending rigidities and subscripts x and y denote partial differentiations.

The double integral in equation (6) covers the area within the ellipse outside of the fastener hole, as shown by the shaded region in Figure 1. The delamination buckling load is obtained by letting the variation of the total potential energy equal to zero, that is

$$\delta (U - W) = 0 \tag{7}$$

where W is the work done by the external load. In the present problem

$$W = \frac{1}{2} \int\int N_x \, w_x^2 \, dxdy \tag{8}$$

Substituting equation (5) into (6) and (8) resulting in 127 integrals in the general form of:

$$I = f(a,b,R) \left\{ \int_{-b}^{-R} \int_{-c_1}^{c_1} x^m y^n \, dxdy \right.$$

$$+ \int_{R}^{b} \int_{c_2}^{c_1} x^m y^n \, dxdy + \int_{-R}^{-R} \int_{-c_1}^{c_2} x^m y^n \, dxdy$$

$$\left. + \int_{-R}^{R} \int_{c_2}^{c_1} x^m y^n \, dxdy \right\} \tag{9}$$

where m and n are positive integers $0 \leq m, n \leq 14$

$$c_1 = \frac{a}{b} \sqrt{b^2 - y^2}$$

$$c_2 = \sqrt{R^2 - y^2}$$

f (a,b,R) is a polynominal in terms of a, b and R.

These lengthy algebraic manipulations were carried out and the results were coded into a computer program operational on personal computers.

Strain Energy Release Rate Computation

The value of the strain energy release rate (G) for an elliptical delamination varies around the periphery of the delamination front. This has

been shown in Reference 1 for laminates with a delamination loaded in compression. The analysis method of Reference 1 is used here for strain energy release rate computation. This method is applicable to both delamination configurations shown in Figures 1 and 2. In Reference 1, the strain energy release rate is computed based on the assumption that the inplane displacement along the lines AA and BB (see Figure 1) is constant through the width of the laminate. The strain energy release rate at a point y on the delamination front due to compression is then given by

$$G_A = \tfrac{1}{2} N_y (N_y - N_{cr}) \left[\frac{1}{E_{xs} t_s} - \frac{1}{E_x t} \right] \tag{10}$$

where N_y is determined based on the assumption that AA and BB remain straight under applied load. The relationship between N_y and the applied compression N is given by

$$N_y = \frac{\dfrac{aN}{t_2 E_{x2}} - (a-d) N_{cr} \left[\dfrac{1}{t_2 E_{x2}} - \dfrac{1}{t E_x} \right]}{\dfrac{d}{t_2 E_{x2}} + \dfrac{a-d}{t E_x}} \tag{11}$$

where

$$d = \frac{a}{b} (b^2 - y^2) \tag{12}$$

is the distance from the delamination centerline to the point of interest along the loading direction.

Similarly, the strain energy release rate due to applied bending moment is given by

$$G_B = \frac{1}{2} \left\{ \left(\frac{M_y - M_{cr}}{D_{11s}} \right)^2 \sum^{n_s} A_{11i} y_{si}^2 + \frac{M_{cr}(M_y - M_{cr})}{D_{11} D_{11s}} \sum^{n_s} 2 A_{11i} y_{si} - \left[\left(\frac{M_y}{D_{11}} \right)^2 - \left(\frac{M_{cr}}{D_{11}} \right)^2 \right] \sum^{n} A_{11i} y_i^2 \right\} \tag{13}$$

In equation (13) M_y, the effective moment, depends on the location of the point of interest. M_y is related to the applied bending moment (M) as

$$M_y = \frac{\frac{aMy_{si}}{D_{11s}} - (a-d)\, M_{cr}\left(\frac{y_{si}}{D_{11s}} - \frac{y_s}{D11}\right)}{\frac{dy_{si}}{D_{11s}} + \frac{(a-d)\, y_s}{D_{11}}} \tag{14}$$

where D_{11} is the bending rigidity of the laminate
D_{11s} is the bending rigidity of the remaining layer (layer 2 in Fig. 1)
y_s is the distance of the first ply beneath the delamination to the laminate neutral axis
y_{si} is the distance of the first ply beneath the delamination to the neutral axis of the remaining layer

The total strain energy release rate is then given by

$$G_T = G_A + G_B \tag{15}$$

Failure Prediction

It was recognized early in the analysis development of Reference 1 that delaminations can cause several different failure modes which all have to be accounted for to predict residual strength correctly. Figure 3 summarizes the six potential failure modes for delaminated laminates. To account for these failure modes, it is necessary to predict:

1. Compression strength of a laminate with delaminations
2. Initial buckling strength
3. Local buckling strength
4. Global buckling strength
5. Laminate compression strength

These strengths are then plotted as a function of the delamination size. From such a plot, the overall laminate strength as a function of delamination size can be determined.

An example of such a plot is shown in Figure 4. In this example, it is assumed that the compression strength of the undamaged laminate is lower than the global buckling strength of the laminate. That is, when there is no delamination present in the laminate, the laminate failure mode is compression failure. When a delamination is introduced, both the failure mode and the failure strength depend on the delamination size. In Figure 4, the lower bound failure strength as a function of the delamination size is shown by a solid line, which can be divided into three regions. In Region I the size of the delamination is small, the initial buckling strength is high, and the failure strength equals the undamaged laminate compression strength (Failure Mode 1). In Region II the initial buckling strength is lower than the

undamaged laminate compression strength. The failure is initiated by initial buckling of the delamination followed by stress redistribution until finally, the compression stress in the remaining layer exceeds its compression strength (Failure Mode 2). In Region III the delamination size is large, the failure starts as initial buckling, and is followed by local buckling of the remaining layer (Failure Mode 5). In addition, the delamination may grow under static loading because of released strain energy (Failure Mode 6). As a result of delamination growth, the laminate may fail in either Mode 2, 4, or 5. Clearly, it is important to account for competing failure mode effects in the analysis of delaminated composite structures.

NUMERICAL RESULTS

A 24-ply, $(\pm 45/90/0/\pm 45/0_2/\pm 45/0_2)_s$ laminate is used as an example for numerical analysis. Results for both solid laminates with an elliptical delamination (Figure 1) and elliptical delamination around a clamp-up fastener hole are obtained. Initial buckling load, strain energy relese rate and failure prediction for each delamination configuration are presented below.

Elliptical Delamination

The initial buckling load for the 24-ply $(\pm 45/90/0/\pm 45/0_2/\pm 45/0_2)_s$ laminate is shown in Figure 5. The figure shows the initial buckling load for the laminate with a 4-ply deep circular delamination with a boundary fixity coefficient of 0. Buckling loads (Ncr) for the N/M ratio of 10, 20, 50 and ∞ are shown in the figure. As can be seen in the figure, the buckling load depends on the axial force to bending moment ratio. The results of Reference 1 are recovered for $N/M = \infty$ (pure compression).

As stated earlier, the value of the strain energy release rate (G) varies around the delamination front. Only the maximum values are shown here, because those values control the growth of the delamination. The maximum strain energy release rate occurs at points along the delamination centerline normal to the loading direction. This result indicates that delamination growth would initiate in the direction normal to the applied load. In other words, the aspect ratio of the delamination (a/b) will decrease as delamination grows. Typical maximum strain energy release rates (G_{max}) are shown in Figures 6 and 7. In these figures the values of G_{max}, under constant laminate load, are plotted as a function of delamination radius. Figure 6 shows the values of G_{max} for a laminate subjected to pure bending with the delamination on the compression side. The values of G_{max} for the 24-ply laminate subjected to compression dominated loading (N/M=50) are shown in Figure 7. Both Figures 6 and 7 show similar trends for the value of G_{max} as a function of delamination size. That is, G_{max} remains zero when the applied load is below delamination buckling load. The value of G_{max} increases sharply following the initial buckling and stabilizes as the delamination size becomes larger.

The variation of G around the delamination front is shown in Figure 8. This figure shows that the variation of G around the delamination is more significant for increased bending (decreased N/M ratio).

The failure load, failure mode and failure sequence of the 24-ply laminate with a 4-ply circular delamination under combined load (N/M=50) are shown in Figure 9. The figure shows the results for a delamination with a boundary fixity coefficient of 0. It can be seen from the figure that, depending on the delamination size, there are four different failure modes. For small delamination, ($R \leq 0.65$ in) the delamination buckling load is high and laminate strength controls the failure of the damaged laminate. As the size of the delamination increases ($0.65 < R < 0.7$), the delamination buckled before failure occurs. However, no delamination growth takes place and the failure is controlled by the undamaged laminate strength. Further increases in delamination size ($0.7 \leq R < 0, 85$), buckling and delamination growth take place prior to final laminate failure. For large delamination ($R \geq 0.85$ in) the failure load is controlled by the strength of the remaining layer. Failure occurs after buckling of the delaminated region and significant growth of the delamination.

Comparisons of observed (Reference 1) and predicted failure strains are shown in Figures 10 through 12. Figure 10 shows the effects of delamination size, shape and depth location on the residual strength of the laminate. The analysis correctly predicted the failure sequence and reasonably predicted the failure strain, except for the 4-ply deep 1.0-inch diameter delamination. For this delamination type, no delamination buckling was predicted. Experimental data, however, showed that buckling occurred at approximately 80% of the failure load. This deficiency may be due to the value of the boundary fixity coefficient chosen in the analysis (0.33).

The influence of the multiple delaminations on the residual strength of the laminate is shown in Figure 11. The figure shows that the analysis overpredicted the failure strain for specimens with three delaminations when α=0.33 was used for all delaminations. However, if the inner sublaminates separated by the near surface and the mid-plane delaminations assumed a less constrained fixity the correlation can be significantly improved. The prediction agrees with experimental data for $\alpha = 0.7$ as shown in Figure 11.

The influence of laminate thickness on residual strength is shown in Figure 12. The analytical correlations are not conclusive because of the large number of tab failures during test of the thicker specimens. However, the predictions are conservative when compared with data for specimens with no tab failure.

Elliptical Delamination Around a Clamped Fastener Hole

The buckling load for an elliptical delamination around a clamped fastener hole (Figure 2) is obtained by using equation (7). After lengthy algebraic manipulations equation (7) is coded into a computer code operational on personal computers. Typical buckling loads based on this analysis method are shown in Figure 13. The figure shows the buckling loads for the 24-ply laminate with a 4-ply deep delamination around a 0.25 in. diameter fastener hole.

Figure 13 shows that the buckling load for this delamination configuration is very high, as compared to the buckling load for a circular delamination of equal size in a solid laminate (also shown in the figure for comparison purposes). This is an indication that for this laminate, smaller delaminations (smaller than 1.5 inches in diameter) failure is controlled by the effects of stress concentration of a filled fastener hole. The effects of delamination on the failure strength is small.

Failure of delaminations around fastener holes are similar to that in a solid laminate. However, because of the stress concentration effects induced by the fastener hole, a hole failure criterion must be used in the failure prediction. The average stress (strain) criterion proposed in Reference 24 with a filled hole correction factor is used in the present program. The average stress criterion predicts the failure stress (strain) of a laminate with an open hole. For a fastener hole with fastener installed, a correction factor of 1.15 is applied. This value of filled hole correction factor is obtained by comparing experimental data generated under a Northrop IRAD program (Reference 25).

The failure analysis method, the buckling analysis method and the strain energy release rate computation technique were integrated into a computer code for strength prediction. Typical results obtained from the computer program are summarized in Figure 14.

Figure 14 shows that the failure mode depends on the delamination size. For a delamination radius from 0.5 to 2.5 inches, there are three distinct failure modes. At a delamination radius up to 1.3 inch, the delamination buckling strength is high, failure of the laminate is governed by the filled hole strength of the delaminated plate. Failure may initiate in the delamination layer or the remaining layer, depending on the stress concentration factor of the respective layer. At a delamination radius of 1.4 inch, the delamination layer buckling strength is lower than the laminate strength. Thus, buckling occurs before the final failure. After the delamination buckled, release of strain energy takes place. However, for this delamination size, the energy release is not sufficient for delamination growth. The laminate failed in the remaining layer without delamination propagation. As the delamination size further increased, delamination growth occurs at load level N_G before the final failure at the filled hole in the remaining layer.

Results for the 24-ply laminate with 1-, 2-, 4- and 6- ply deep delamination are shown in Figure 15. The figure shows that for each delamination depth, there is a clear transition in failure mode. At a smaller delamination size, the failure mode is a filled hole strength failure with no buckling or delamination growth (mode 1 in Figure 14). With larger delamination, the mode of failure becomes a remaining layer hole failure after delamination buckling (with or without delamination growth, mode (2) or (3) in Figure 14).

SUMMARY

A methodology has been developed for strength prediction of composite structures with imbedded delaminations under combined bending and compression loads. The methodology is further modified to accommodate the presence of a fastener through an elliptical delamination by modelling the effects of fastener clamping force. Limited data correlation indicates that the methodology correctly predicts the failure load and failure sequence of delaminated composite laminates. Further verification of the methodology is currently being conducted under a NADC/FAA/Northrop contract N62269-90-C-0282, entitled "Delamination Methodology for Composite Structures".

REFERENCES

1. Horton, R. E., Whitehead, R. S., et al, "Damage Tolerance of Composites" AFWAL-TR-87-3030, Vol. I, II, and III, July 1988.

2. Kachanov, L. M., "Separation Failure of Composite Materials," Polymer Mechanics, Vol. 12, 1976, pp. 812-815.

3. Whitcomb, J. D., "Finite Element Analysis of Instability-Related Delamination Growth," Journal of Composite Materials, Vol. 15, September 1981, pp. 403-426.

4. Whitcomb, J. D., "Strain-Energy Release Rate Analysis of Cyclic Delamination Growth in Compressively Loaded Laminates," Effects of Defects in Composite Materials, ASTMSTP 836, American Society for Testing and Materials, 1984, pp. 175-193.

5. Chai, H., Babcock, C. D., and Knauss, W. G., "One Dimensional Modelling of Failure in Laminated Plates by Delamination Buckling," International Journal of Solids and Structures, Vol. 18, 1981, pp. 10.

6. Wang, S. S., Zahlan, N. M. and Suemasu, H., "Compressive Stability of Random Short-Fiber Composites, Part II - Experimental and Analytical Results," Journal of Composite Materials, Vol. 19, July 1985, pp. 317-333.

7. Ashizawa, M., "Fast Interlaminar Fracture of a Compressively Loaded Composite Containing a Defect," Proceedings of the Fifth DOD/NASA Conference on Fibrous Composites in Structural Design, New Orleans, Louisiana, January 1981.

8. Simitses, G. J., Sallam, S., and Yin, W. L., "Effect of Delamination of Axially Loaded Homogeneous laminated Plates," AIAA Journal, Vol. 23, 1985, pp. 1437-1444.

9. Sallam, S., and Simitses, G. J., "Delamination Buckling and Growth of Flat, Cross-Ply Laminates," Composite Structures, Vol. 4, 1985, pp. 361-381.

10. Konishi, D. Y., and Johnson, W. R., "Fatigue Effects on Delaminations and Strength Degradation in Graphite/Epoxy Laminates," Composite Materials: Testing and Design Fifth Conference, ASTM STP 674, American Society for Testing and Materials, 1979, pp. 597-619.

11. Chai, H., "The Growth of Impact Damage in Compressively Loaded Laminates," PhD Thesis, California Institute of Technology, March 1982.

12. Chai, H., and Babcock, C. D., "Two-Dimensional Modelling of Compressive Failure in Delaminated Laminates," Journal of Composite Materials, Vol. 19, January 1985, pp. 67-98.

13. Webster, J. D., "Flaw Criticality of Circular Disbond Defects in Compressive Laminates," Center for Composite Materials Report No. 81-03, 1981.

14. Shivakumar, K. N., and Whitcomb, J. D., "Buckling of a Sublaminate in a Quasi-Isotropic Composite Laminate," Journal of Composite Materials, Vol. 19, January 1985, pp. 2-18.

15. Whitcomb, J. D., and Shivakumar, K. N., "Strain Energy Release Analysis of a Laminate With a Postbuckled Delamination," Fourth International Conference on Numerical Methods in Fracture Mechanics, Pineridge Press, 1987, pp. 581-605.

16. Yin, W. L., "Axisymmetric Buckling and Growth of a Circular Delamination in a Compressed Laminate," International Journal of Solids and Structures, Vol. 21, 1985, pp. 503-514.

17. Fei, Z., and Yin, W., "Postbuckling Growth of a Circular Delamination in a Laminate Under Compression and Bending," Proceedings of SECTAM XII, Vol. II, May 1984, pp. 130-134.

18. Whitcomb, J. D., "Instability-Related Delamination Growth of Embedded and Edge Delaminations," NASA TM 100655, August 1988.

19. Marshall, R. D., Sandorff, P. E., and Laruaitis, K. N., "Buckling of a Damaged Sublaminate in an Impacted Laminate," Journal of Composites Technology and Research, Vol. 10, No. 3, 1988, pp. 107-113.

20. Ramkumar, R. L., "Fatigue Degradation in Compresively Loaded Composite Laminates," NASA CR 165681, April 1981.

21. Ramkumar, R. L., "Performance of a Quantitative Study of Instability-Related Delmaination Growth," NASA CR 166046, March 1983.

22. Byers, B. A., "Behavior of Damaged Graphite/Epoxy Laminates Under Compression Loading," NASA CR 159293, August 1980.

23. Porter, T. R., "Compression and Compression Fatigue Testing of Composite Laminates," NASA CR 168023, 1982.

24. Whitney, J. M. and Nuismer, R. J., "Stress Fracture Criteria for Laminated Composites Containing Stress Concentrations," Journal of Composite Materials, Volume 8, 1974.

25. Whitehead, R. S., et al., "Advanced Material Development Program," Northrop IRAD D-1913, 1986-1991.

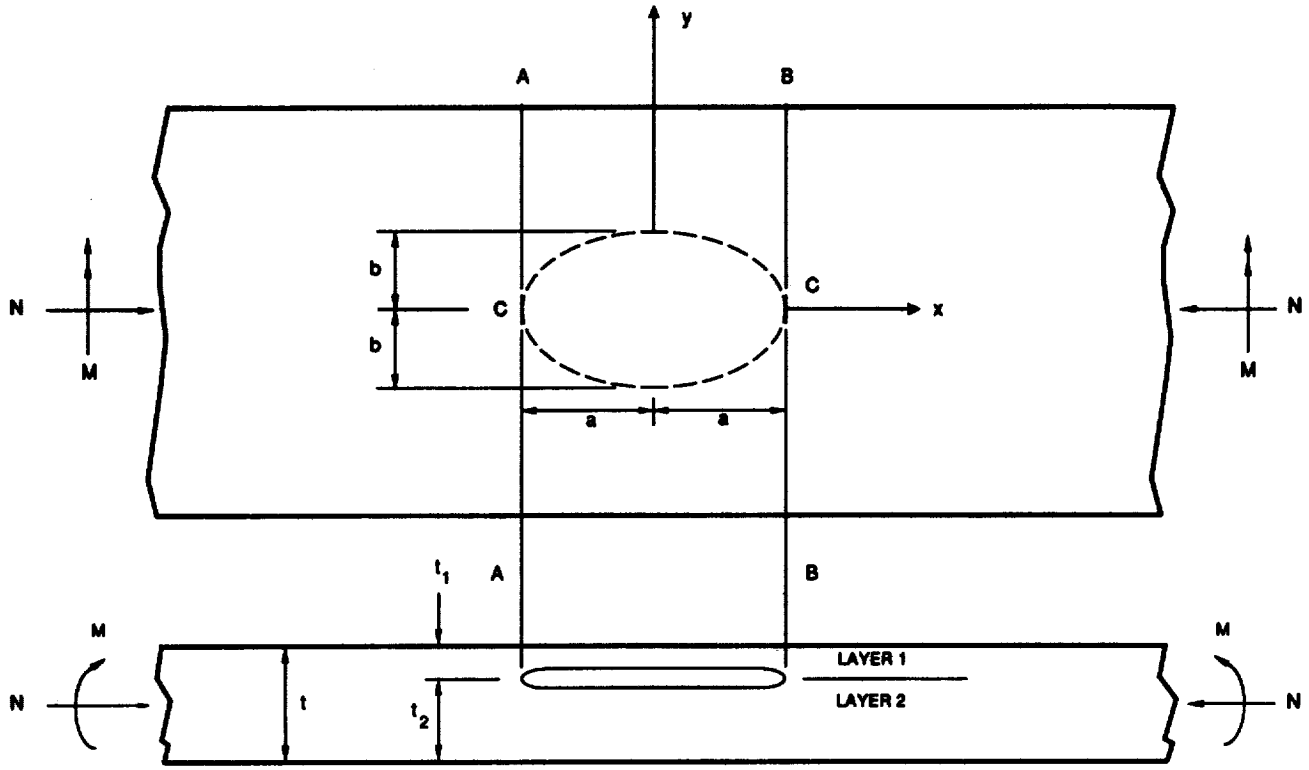

Figure 1. Laminate With an Elliptical Delamination.

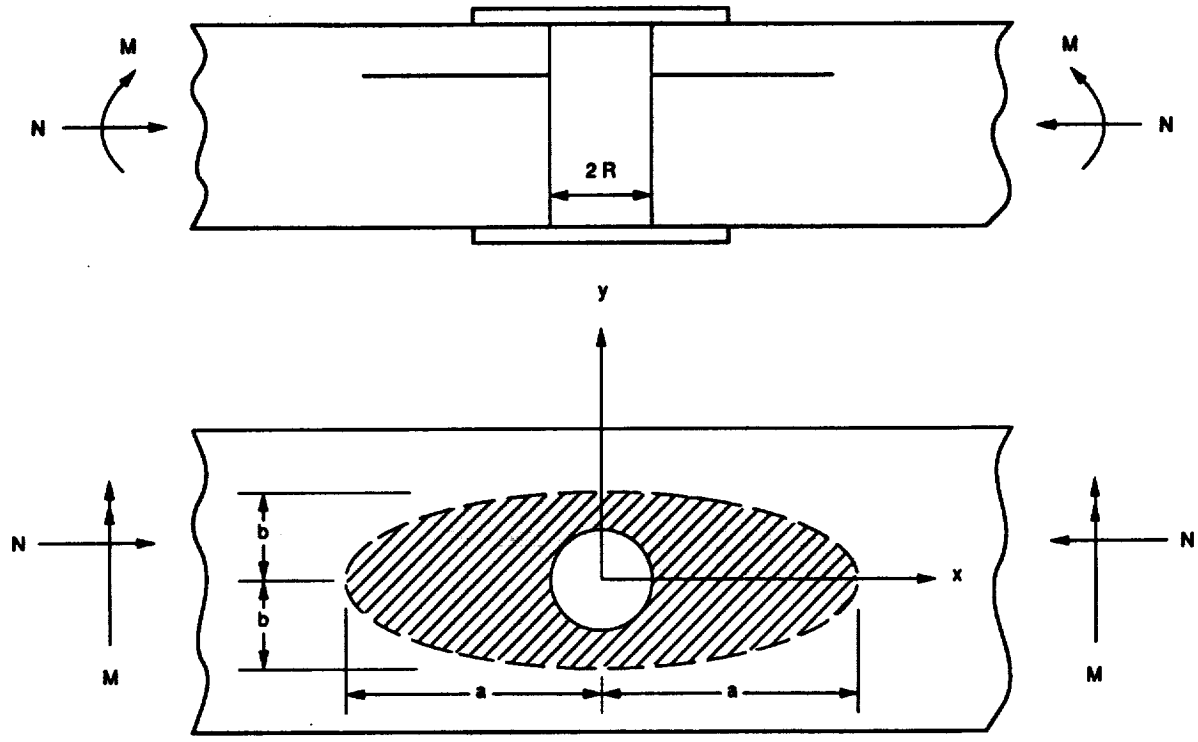

Figure 2. Delamination Around a Fastener Hole.

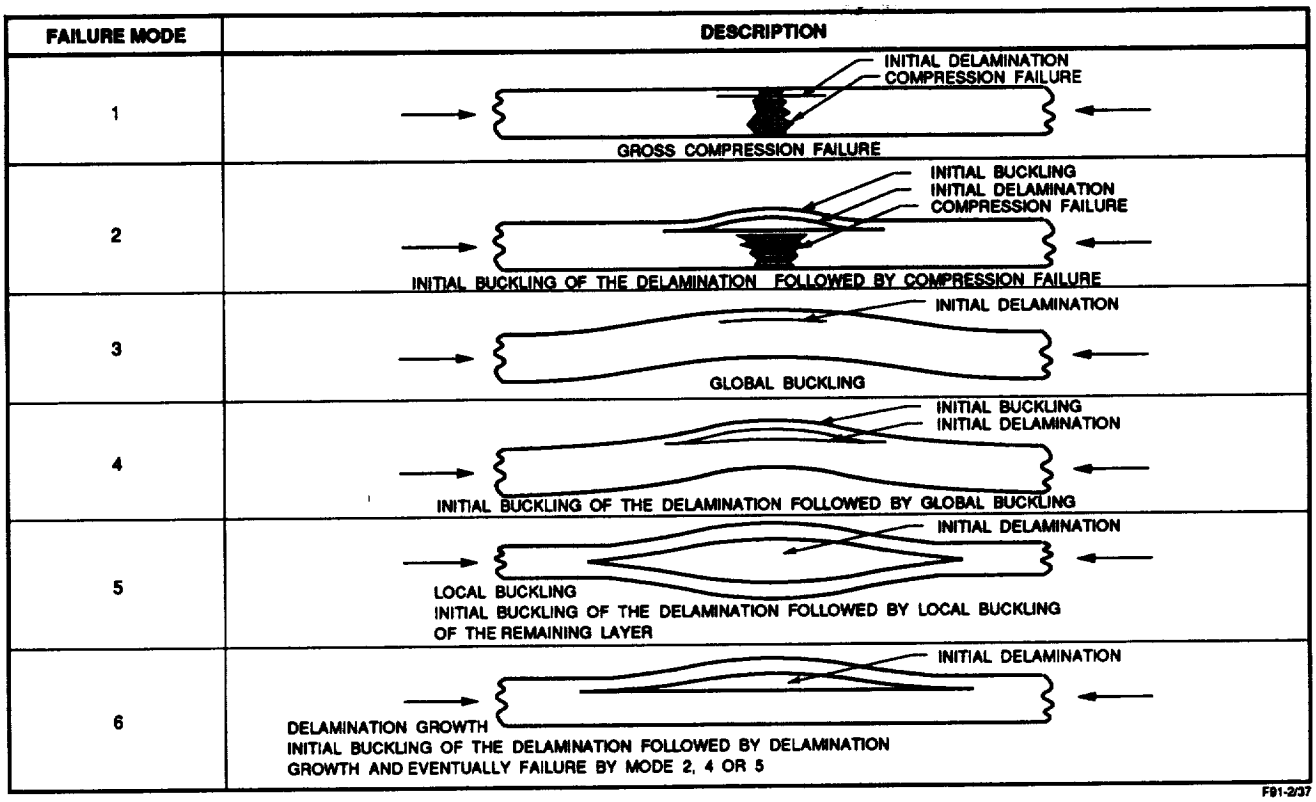

Figure 3. Static Failure Modes for a Laminate With Delamination.

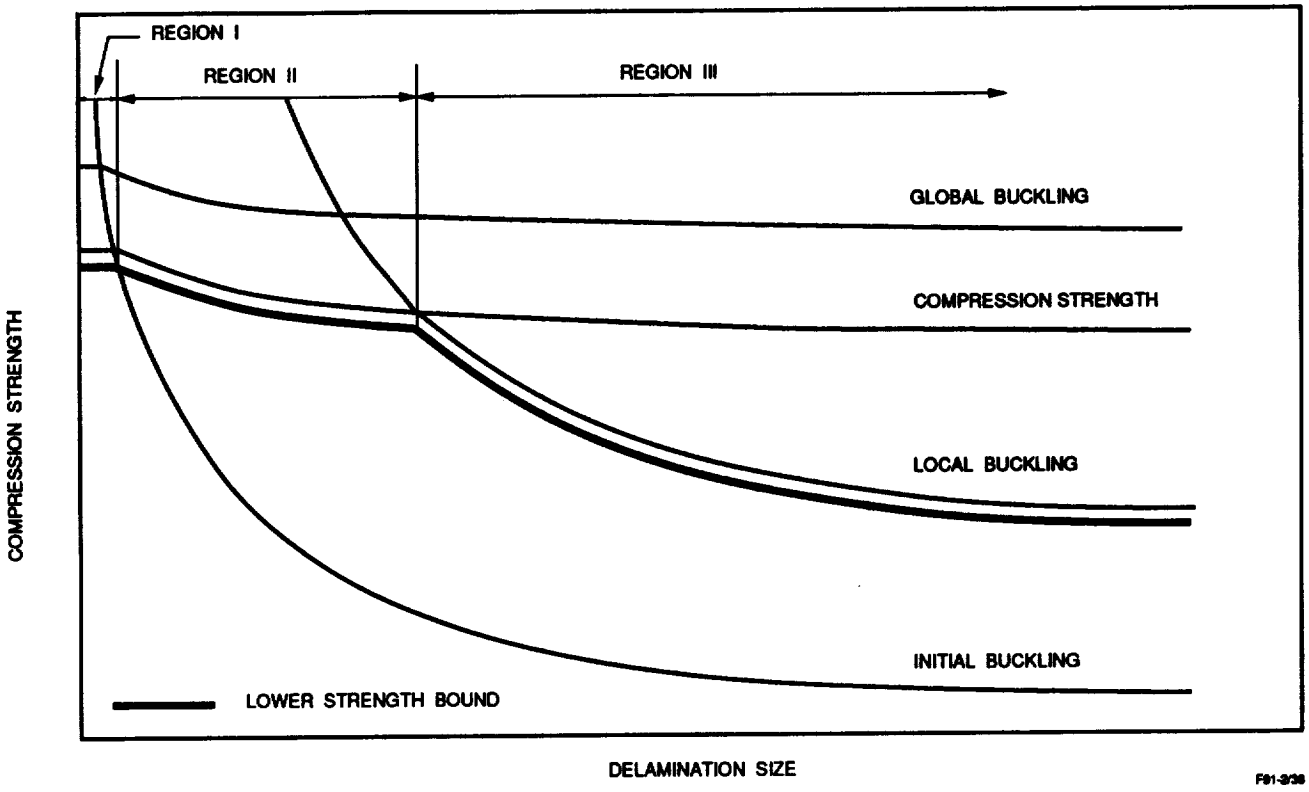

Figure 4. Failure Mode and Failure Strength Dependence on Delamination Size.

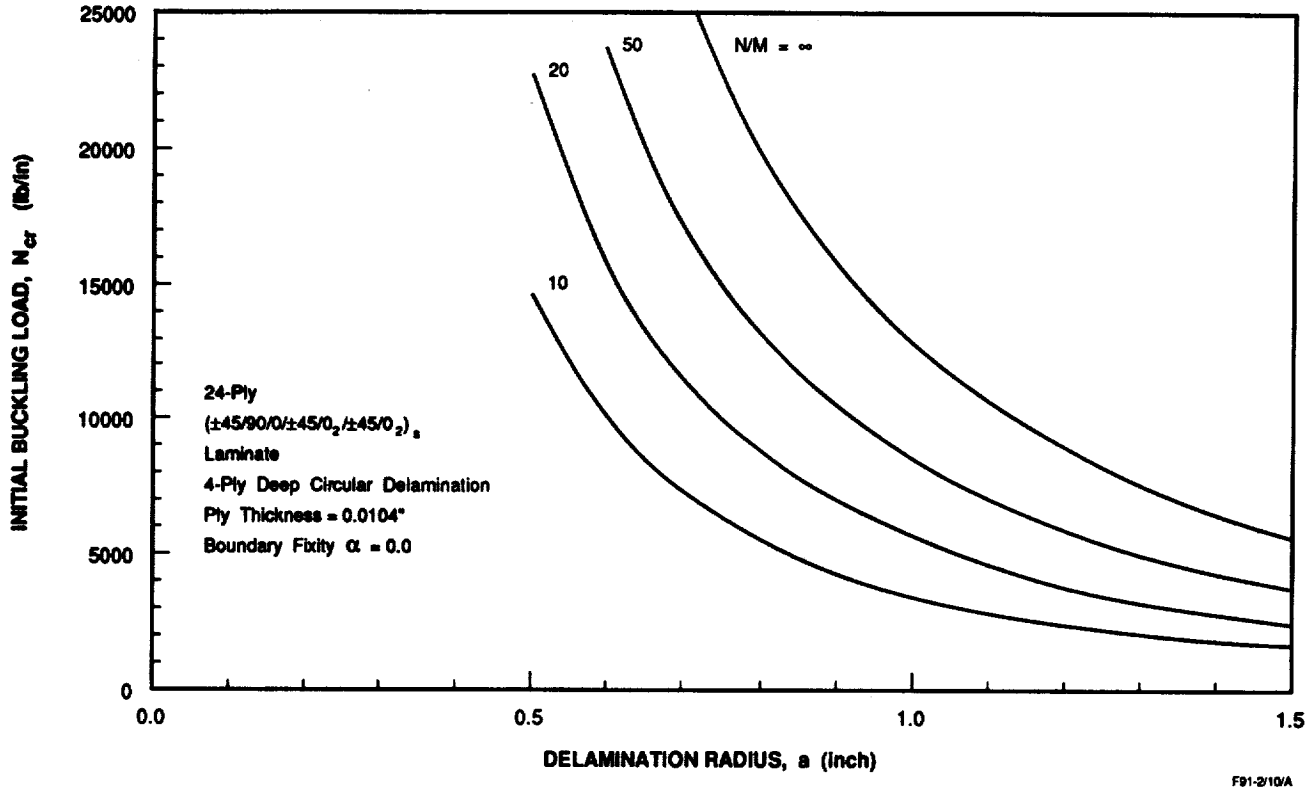

Figure 5. Initial Buckling Load for a 24-Ply Laminate With a Circular Delamination.

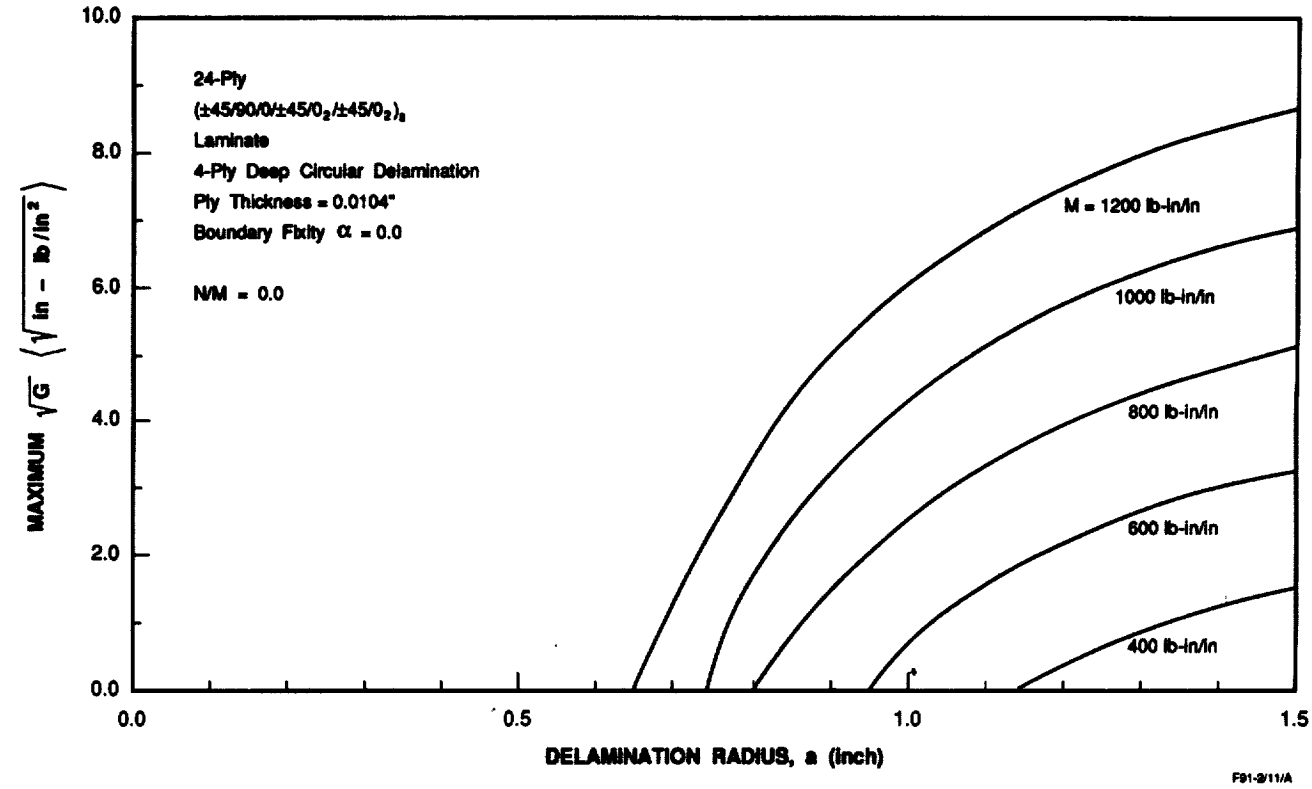

Figure 6. Strain Energy Release Rate for a 24-Ply Laminate With a Circular Delamination – Pure Bending.

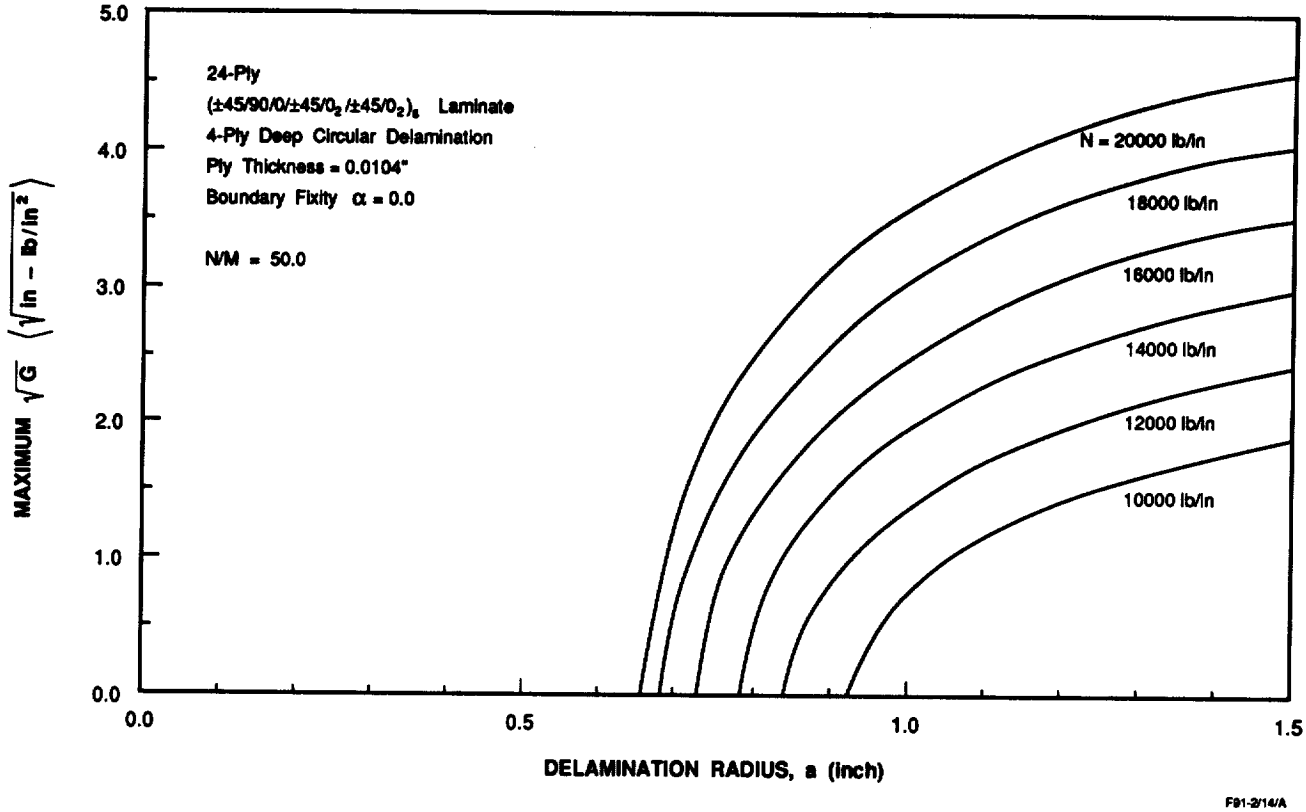

Figure 7. Strain Energy Release Rate for a 24-Ply Laminate With a Circular Delamination Under Combined Compression and Bending Loads – N/M = 50.0.

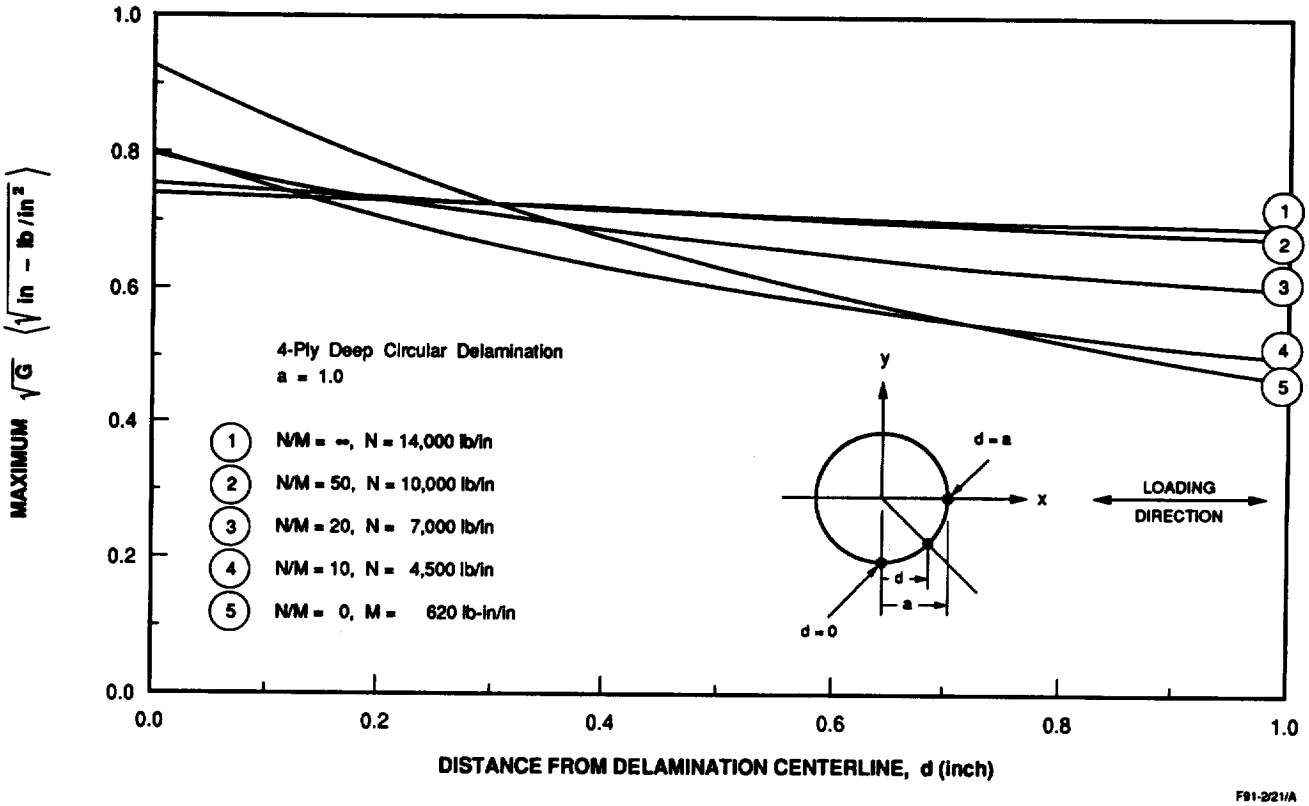

Figure 8. Strain Energy Release Rate Around the Periphery of a Circular Delamination.

DELAMINATION RADIUS R (in)	BUCKLING LOAD N_{cr} (lb/in)	FAILURE LOAD N_f (lb/in)	FAILURE MODE
0.5	29,074	17,800	(1)
0.6	20,191	17,800	(1)
0.65	17,204	17,800	(2)
0.7	14,834	17,800	(3) N_G = 16,239
0.8	11,357	17,800	(3) 13,035
0.9	8,974	17,337	(4) 10,893
1.0	7,269	16,924	(4) 9,394
1.1	6,007	16,618	(4) 8,307
1.2	5,048	16,385	(4) 7,493
1.3	4,301	16,204	(4) 6,868
1.4	3,708	16,061	(4) 6,379
1.5	3,230	15,945	(4) 5,987
1.6	2,839	15,850	(4) 5,669
1.7	2,515	15,771	(4) 5,408
1.8	2,243	15,706	(4) 5,190
1.9	2,013	15,650	(4) 5,006
2.0	1,817	15,602	(4) 4,850
2.1	1,648	15,561	(4) 4,716
2.2	1,502	15,526	(4) 4,601
2.3	1,374	15,495	(4) 4,500
2.4	1,262	15,468	(4) 4,412
2.5	1,163	15,444	(4) 4,334

UNDAMAGED LAMINATE STRENGTH: N = 17,800 lb/in, M = 356 lb-in/in

UNDAMAGED REMAINING LAYER STRENGTH: N = 15,160 lb/in, M = 303 lb-in/in

FAILURE MODES:

(1) NO BUCKLING, NO DELAMINATION GROWTH, FAILED BY LAMINATE STRENGTH.

(2) DELAMINATION BUCKLED, NO DELAMINATION GROWTH, FAILED BY LAMINATE STRENGTH.

(3) DELAMINATION BUCKLED AND GROWN AT N_G , FAILED BY REMAINING LAYER STRENGTH.

F91-2/40

Figure 9. Failure Load and Mode of the 24-Ply Laminate With a 4-Ply Deep Circular Delamination Under Combined Loads (N/M = 50).

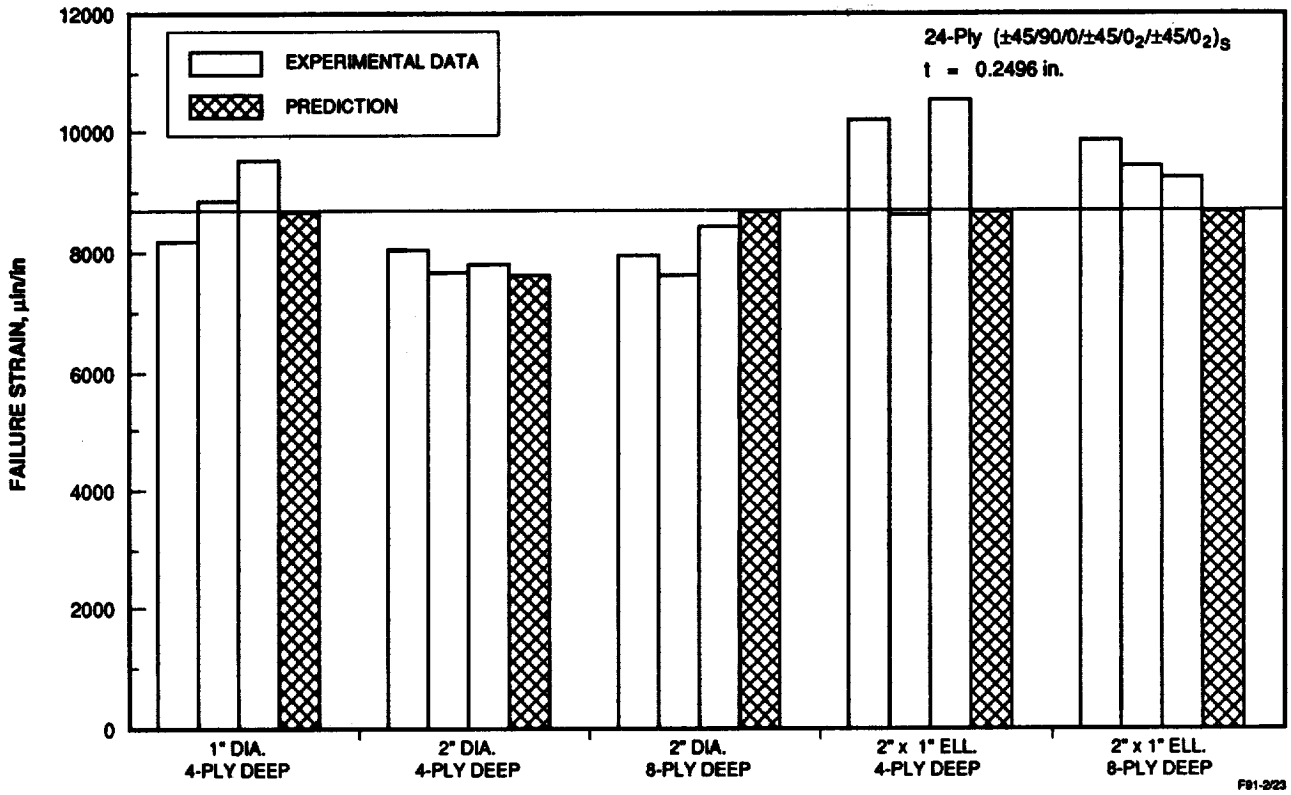

Figure 10. Comparison of Observed and Predicted Failure Strain of a 24-Ply Laminate With Single Circular or Elliptical Delamination.

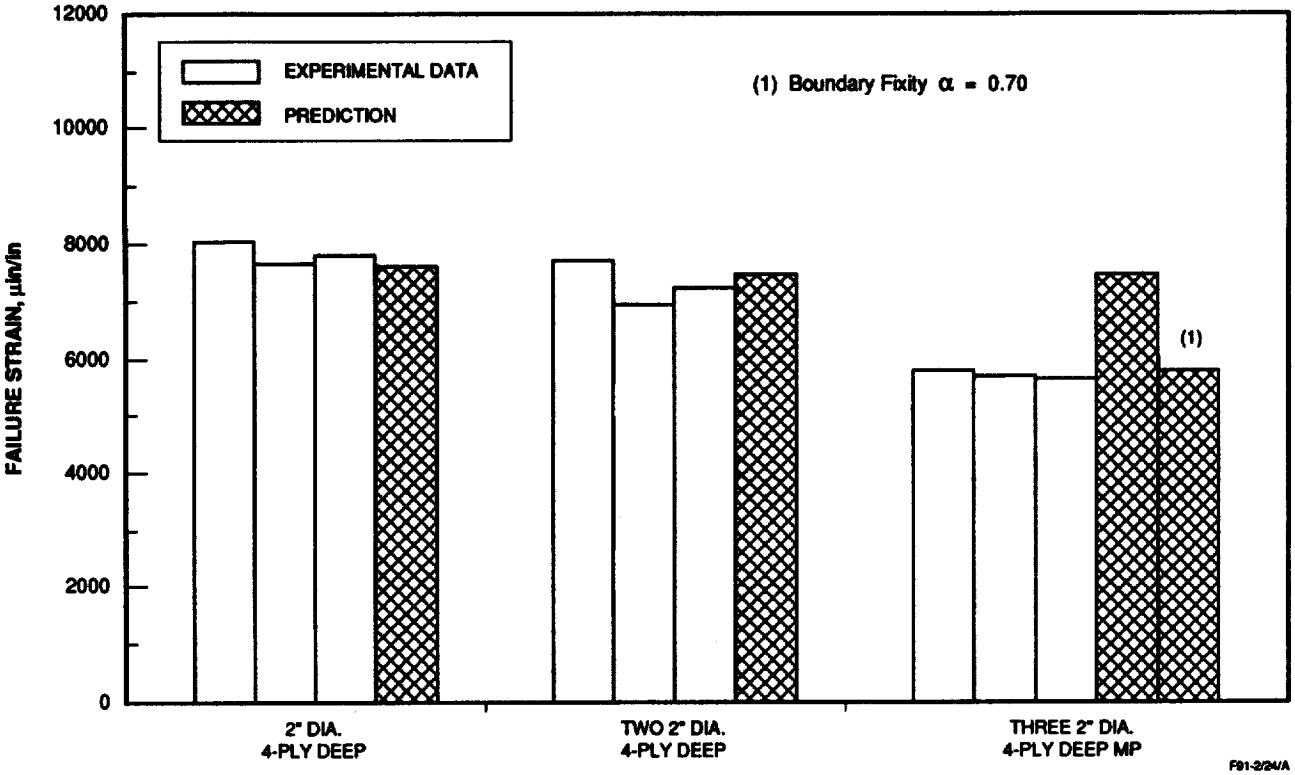

Figure 11. Comparison of Observed and Predicted Failure Strain of a 24-Ply Laminate With Multiple Delaminations.

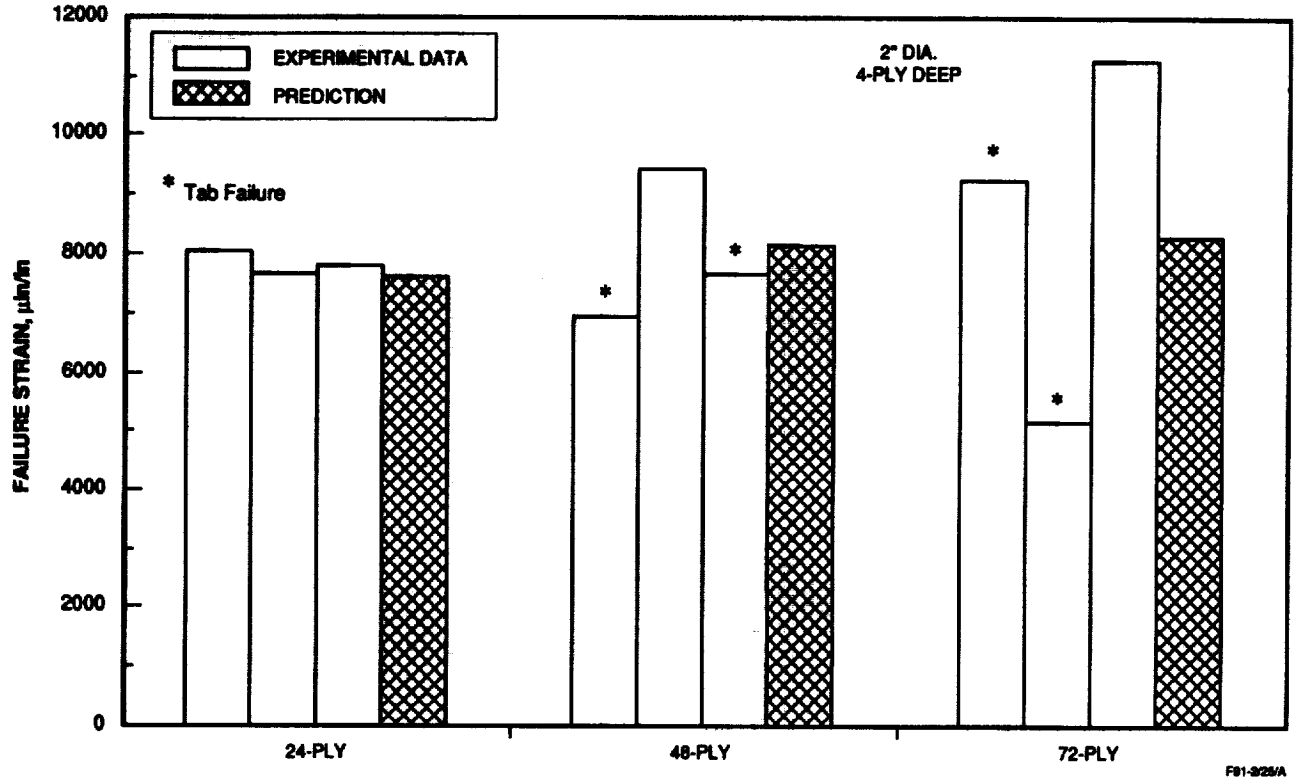

Figure 12. Comparison of Observed and Predicted Failure Strain for Laminate With 4-Ply Deep Circular Delamination.

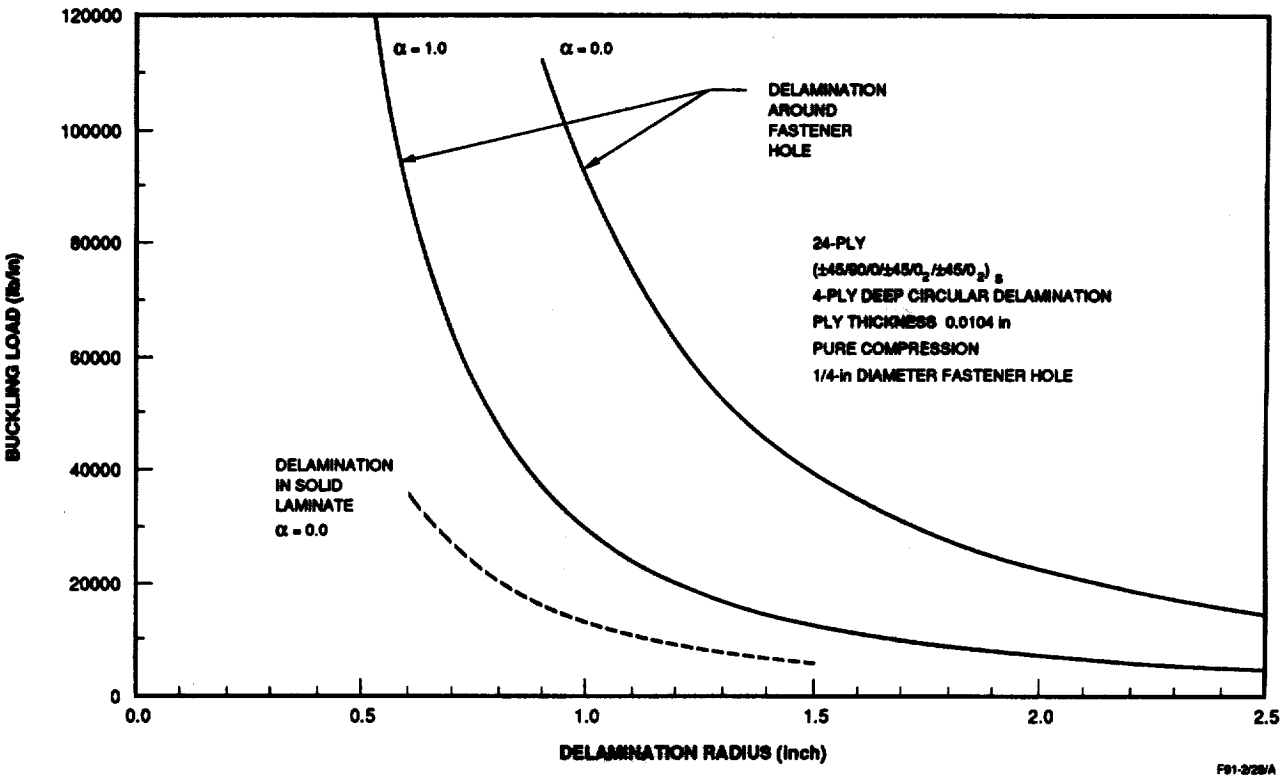

Figure 13. Initial Buckling Load for Delamination Around a Fastener Hole.

DELAMINATION RADIUS R (in)	BUCKLING LOAD N_{cr} (lb/in)	FAILURE LOAD N_f (lb/in)	FAILURE MODE
0.5	129,220	16,455	(1)
0.6	86,590	16,455	(1)
0.7	62,320	16,455	(1)
0.8	47,090	16,455	(1)
0.9	36,880	16,455	(1)
1.0	29,690	16,455	(1)
1.1	24,420	16,455	(1)
1.2	20,450	16,455	(1)
1.3	17,380	16,455	(1)
1.4	14,950	15,590	(2)
1.5	13,000	15,440	(3) N_G = 14,630
1.6	11,410	15,310	(3) 13,210
1.7	10,100	15,210	(3) 12,060
1.8	8,998	15,120	(3) 11,120
1.9	8,069	15,050	(3) 10,340
2.0	7,278	14,980	(3) 9,688
2.1	6,597	14,930	(3) 9,140
2.2	6,008	14,880	(3) 8,676
2.3	5,494	14,840	(3) 8,279
2.4	5,044	14,810	(3) 7,937
2.5	4,647	14,780	(3) 7,640

LAMINATE STRENGTH: SOLID 25,920 lb/in
FILLED HOLE 16,600 lb/in
FILLED HOLE WITH DELAMINATION 16,455 lb/in

REMAINING LAYER STRENGTH: SOLID 22,700 lb/in
FILLED HOLE 14,410 lb/in

FAILURE MODE:
(1) NO BUCKLING, NO DELAMINATION GROWTH, FAILURE DUE TO STRESS CONCENTRATION AT FILLED HOLE.
(2) DELAMINATION BUCKLED, NO DELAMINATION GROWTH, FAILURE AT FILLED HOLE IN THE REMAINING LAYER.
(3) DELAMINATION BUCKLED AND GROWN AT N_G THAN FAILED AT FILLED HOLE IN THE REMAINING LAYER.

F91-2/39

Figure 14. Results of Failure Analysis.
4-Ply Deep Circular Delamination in 24-Ply Laminate
0.25 in Diameter Fastener Hole

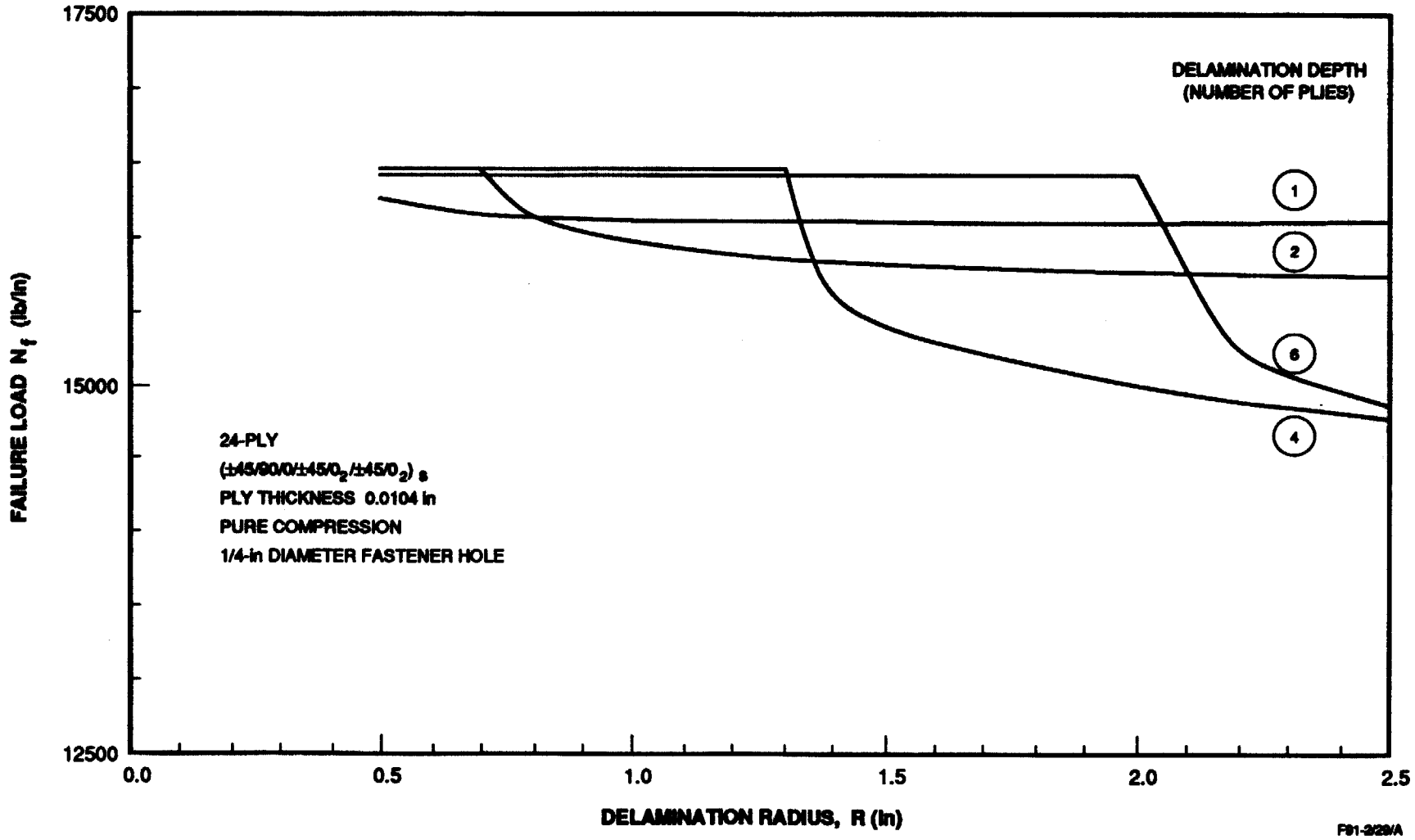

Figure 15. Failure Load of Laminate With Circular Delaminations Around a Fastener Hole.

Omit

Mechanics of Composites Research at ONR

Yapa D. S. Rajapakse
Office of Naval Research

THIS PAGE INTENTIONALLY BLANK

omit

Post-Buckling Analysis of Curved, Stiffened Composite Panels with Central Cut-Outs

U. Mbanefo
Northrop Corporation

THIS PAGE INTENTIONALLY BLANK